Nuclear Inst. and Methods in Physics Research, A 916 (2019) 1–7

Contents lists available at ScienceDirect

Nuclear Inst. and Methods in Physics Research, A

journal homepage: www.elsevier.com/locate/nima

A method for determining the angular distribution of atmospheric muons using a cosmic ray telescope

M. Bahmanabadi

Department of Physics, Sharif University of Technology, P.O. Box 11155-9161, Tehran, Iran

ARTICLE INFO

Keywords:
Cosmic rays telescope
Atmospheric muon

ABSTRACT

A cosmic ray telescope consisting of two scintillators (each one with a surface area of 0.14 m^2, spaced 283 cm top of each other) was constructed to study the angular distribution of atmospheric muons. Using the CORSIKA code, the muons energy spectrum is parameterized in different energy regions at Tehran's altitude (1200 m above sea level ≡ 897 gcm^{-2}), and by using a Monte Carlo program, the minimum energy recorded by the telescope is calculated. Due to the geomagnetic field, in the azimuth angle distribution of atmospheric muons, an anisotropy is observed in the East–West direction. The zenith angle distribution of the atmospheric muons follows the function $\cos^n\theta$. Due to the relatively large field of view of the telescope, the iteration method is used to obtain the effective angle of orientation of the telescope. With this method, the value $n = 2.33 \pm 0.11$ is calculated. The simulation data also provides the mean value $\bar{n} = 2.30 \pm 0.10$, which has a good match with the experimental result.

1. Introduction

Atmospheric muons are usually a component of extensive air showers (EAS) created by the interaction of primary particles such as protons, alpha, and heavier nuclei with air nuclei. The muons produced from gamma rays are very small compared to cosmic rays that are mainly proton. The abundance of different types of cosmic rays in atmosphere depends on energy. On average, about 90% of atmospheric cosmic rays are protons. But, muons are a dominant component at sea level. Muons observed by cosmic ray detectors located at the ground level are originated from the decay of pions and kaons, which are themselves generated by the interaction of cosmic ray primary particles with the air nuclei. Pion and Kaon mesons both interact and decay in the atmosphere. The prevalence of decay or interaction depends on which of the values energy of meson, E, or $\epsilon = \frac{h_0 mc^2}{c\tau}$ is greater [1]. Where $h_0 = 6.4$ km, m and τ are respectively the mass and mean lifetime of the meson, and c the speed of the light. For $\epsilon \gg E$, decay is dominant and interaction can be ignored [1]. Rest energy and life time of pion and kaon are (139.570 MeV, 26 ns) and (493.688 MeV, 12 ns) respectively, so we obtain $\epsilon_{pion} = 115$ GeV and $\epsilon_{kaon} = 878$ GeV. Therefore, for energies below $E = 10$ GeV, the condition ($\epsilon \gg E$) is valid and the interaction can be ignored. In the air showers, the following interactions produce atmospheric muons:

$$A_{CR} + A_{Air} \rightarrow \pi^{\pm},\ \pi^0,\ k^{\pm},\ \text{other hadrons} \quad (1)$$

$$\pi^{\pm} \rightarrow \mu^{\pm} + \nu_{\mu}(\bar{\nu}_{\mu}) \ \sim 100\% \quad \tau_0 = 26\ \text{ns} \quad (2)$$

$$k^{\pm} \rightarrow \mu^{\pm} + \nu_{\mu}(\bar{\nu}_{\mu}) \ \sim 63.5\% \quad \tau_0 = 12\ \text{ns} \quad (3)$$

Generated muons are usually not proliferated. Usually atmospheric muons do not multiply, but lose their energy by interacting with air nuclei through ionization as they traverse in the atmosphere. The number of muons in a shower increases up to a maximum and then decreases very slowly, While electrons are rapidly reduced after the maximum.

The presence of muons at sea level shows the effects of special relativity. muons have rest energy $m_{\mu}c^2$ of 105.7 MeV and rest frame lifetime $\tau \approx 2.2$ μs. Experimental evidence indicates, however, that muons are produced at high altitude in the atmosphere, with travel time to sea level much greater than τ in the rest frame of the Earth. According to relativity, a muon with $E = 1$ GeV has $\gamma \approx 9.5$. Hence, the lifetime of the muon, as seen from the Earth, is $\gamma\tau \approx 21$ μs, allowing 1 GeV muons to reach the Earth's surface from a height of over $h = c(\gamma^2 - 1)^{0.5}\tau \approx 6$ km.

To measure the muons flux, a cosmic ray telescope has been made at Sharif University of Technology in Tehran (35°43′N, 51°20′E). The elevation of the site is 1200 m above sea level (897 g cm^{-2}). In our previous paper [2], which was studied the muon ratio, we also discussed the zenith and azimuth angles of muons, but in this paper, by providing a suitable method, a detailed analysis of the angular distribution of atmospheric muons is carried out with a new set of data. In the present paper, we have shown the dependence of the muon fluxes on the zenith and azimuth angles for 12 different directions including the North, West, South, and East and in the zenith angles of 20° ± 10°, 40° ± 10°, and 60° ± 10° in energy more than 0.76 GeV. The dependence of the muon flux on the azimuth angle was studied at zenith angles 20°, 40°, and

E-mail address: bahmanabadi@sharif.edu.

https://doi.org/10.1016/j.nima.2018.11.010
Received 29 July 2018; Received in revised form 2 November 2018; Accepted 2 November 2018
Available online 9 November 2018
0168-9002/© 2018 The Author. Published by Elsevier B.V. This is an open access article under the CC BY license (http://creativecommons.org/licenses/by/4.0/).

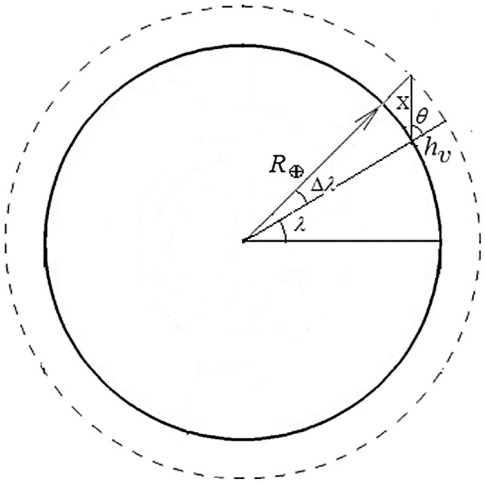

Fig. 1. A schematic of the Earth and atmosphere for showing the angles and notations used in the text.

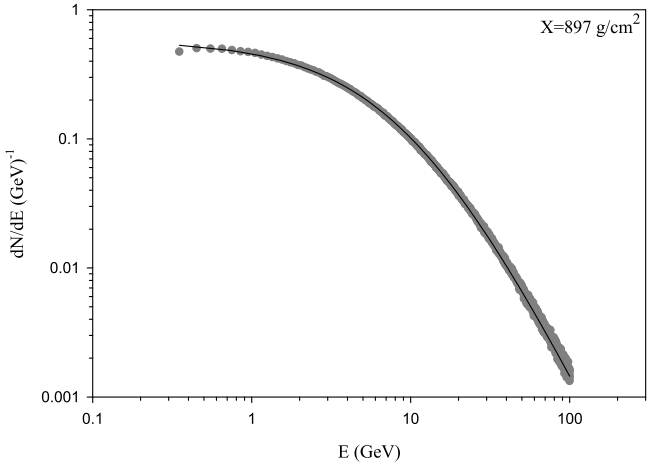

Fig. 2. Energy distributions of the muons at Tehran's level and solid line shows the fitting of Eq. (6).

60°. The effect of the East–West in the flux of muons is also analyzed by considering the geomagnetic field [3].

2. Simulation of the muons energy spectrum

Since our experiments were carried out at Sharif University of Technology in Tehran, IRAN, (34°43′N, 51°20′E; 1200 m a. s. l. ≡ 897 g cm^{-2}), the air showers simulated with the CORSIKA package [4] for study of the muon component were done for this site. CORSIKA (COsmic Ray SImulations for KAscade) simulates EAS initiated by photon and cosmic ray particles, such as proton, alpha, and so on. Different hadronic interaction models are available in CORSIKA. In this work we used the QGSJET (qgsjet01.f package) [5] and GHEISHA (Gamma Hadron Electron Interaction SHower code) [6] models, for hadronic interactions above and below $E_{lab} > 80$ GeV respectively. In the coordinates of the experimental site (Tehran), the components of the geomagnetic field are $B_x = 27.97$ μT, $B_z = 39.45$ μT, which are taken from NOAA's National Centers for Environmental Information (NCEI) [7]. We assume that the geomagnetic field is constant and independent of the angular direction of the muon. To explain this point, consider Fig. 1. Simply we have:

$$h_v \simeq X cos\theta + \frac{X^2}{2R_\oplus} sin^2\theta, \qquad (X/R_\oplus \ll 1). \tag{4}$$

where h_v is vertical altitude of atmosphere, and $X(\theta)$ length of a slant trajectory. For θ less than 60° we can neglect the second term in Eq. (4). If, according to Fig. 1, the latitude of the observation site is λ, the variation in the latitude value of the starting point of muon, $\Delta\lambda$, with the zenith angle θ is given by the following equation:

$$sin(\Delta\lambda) = X(\theta)\frac{sin\theta}{h_v + R_\oplus}. \tag{5}$$

With approximation $X \simeq h_v/cos\theta$, for values $\theta = 60°$, $h_v \simeq 20$ km, and $R_\oplus = 6400$ km, we obtain $\Delta\lambda \simeq 0.3°$. With this value $\Delta\lambda$, the relative variation of the geomagnetic field components at the location of the telescope (Tehran) is calculated. With first order approximation we take the geomagnetic field as a dipole, i.e. $\mathbf{B} = (3(\mathbf{b}\cdot\mathbf{x})\mathbf{x} - x^2\mathbf{b})/x^5$ where b has intensity $b \approx 8\times10^{15}$ Tm^3. So, we get $|\frac{\Delta B_x}{B_x}| = 0.003$, and $|\frac{\Delta B_z}{B_z}| = 0.007$. With these small errors, it can be concluded that a fixed geomagnetic field is a fairly good presumption. Energy of the primary particles was considered between 1 TeV and 1 PeV with a differential flux distribution as $dN/dE \propto E^{-2.7}$. These simulations are in all azimuth angles and for zenith angles of up to 60°. Proton, alpha, and carbon are considered as primary particles with fractions of 87%, 12%, and 1% [8], respectively, for the production of muons in the simulation. The spatial distribution of primary particles is taken isotropic at top of the atmosphere.

A total of 3×10^5 EASs were simulated. The mean energy distribution of the muons produced in the EAS simulations at Tehran's level is as shown in Fig. 2. This energy spectrum, $\frac{dN}{dE}$, in different energy intervals may be parameterized with the following function.

$$\frac{dN}{dE} = k\frac{(E_0 + E)^{-\eta}}{1 + \frac{E}{\epsilon}}. \tag{6}$$

where the parameters k, E_0, η, and ϵ are found by fitting. In Fig. 2, the solid curve shows the fitting of function (6) on the muons spectrum at the level of Tehran. The fit parameters are $k = 166.8 \pm 37.9$ (GeV)$^{\eta-1}$, $E_0 = 9.8 \pm 0.3$ GeV, $\eta = 2.5 \pm 0.1$, and $\epsilon = (8 \pm 2)\times10^3$ GeV, respectively with a regression 99.9%.

Using the equation $E = m_\mu c^2\gamma$ with $\gamma = (1 - \frac{v^2}{c^2})^{-0.5}$, we can write the muon velocity distribution as below,

$$\frac{dN}{dv} = k\frac{(E_0 + m_\mu c^2\gamma)^{-\eta}}{1 + \frac{m_\mu c^2\gamma}{\epsilon}} m_\mu c^2\gamma^3 v. \tag{7}$$

For a given mean path length l, Eq. (7) may be converted into an expected timing distribution, as the experiment described in Section 3.

$$n(t_b)\Delta t_b = k\frac{\left[E_0 + m_\mu c^2(1 - \frac{l^2}{t_b^2c^2})^{-0.5}\right]^{-\eta}}{1 + \frac{m_\mu c^2(1-\frac{l^2}{t_b^2c^2})^{-0.5}}{\epsilon}} m_\mu c^2(1 - \frac{l^2}{t_b^2c^2})^{-1.5} l^2 t_b^{-3}\Delta t_b, \tag{8}$$

where $n(t_b) = \frac{dN}{dt_b}$, $t_b = \frac{l}{v}$ is the time corresponding to a given bin, and Δt_b is the bin width. In a coincidence experiment, a part of the spectral width is related to the velocity of the particle passing through a cosmic ray telescope, which appears as Eq. (8) and is referred to in the data analysis section.

3. Description of the experiments

The cosmic ray telescope consists of two plastic scintillator paddles (100 × 14 × 1 cm^3) spaced 283 cm from each other. Fig. 3 shows a schematic representation of telescope and the electronic device used in this experiment. The data recording operation begins when an muon passes through the top and bottom scintillation detectors. The signals generated in photomultiplier tubes (PMT, 9813B with diameters of 5 cm) viewing the scintillators are amplified 10 times with a fast amplifier (CAEN N412). The signals are then connected to an eight-channel fast discriminator (CAEN N413A), with a threshold level of −20 mV. The outputs of the discriminators were used to create inputs for the START and STOP lines of a time to amplitude converter (TAC, ORTEC 566), which was set to a full scale of 200 ns. TAC output is a

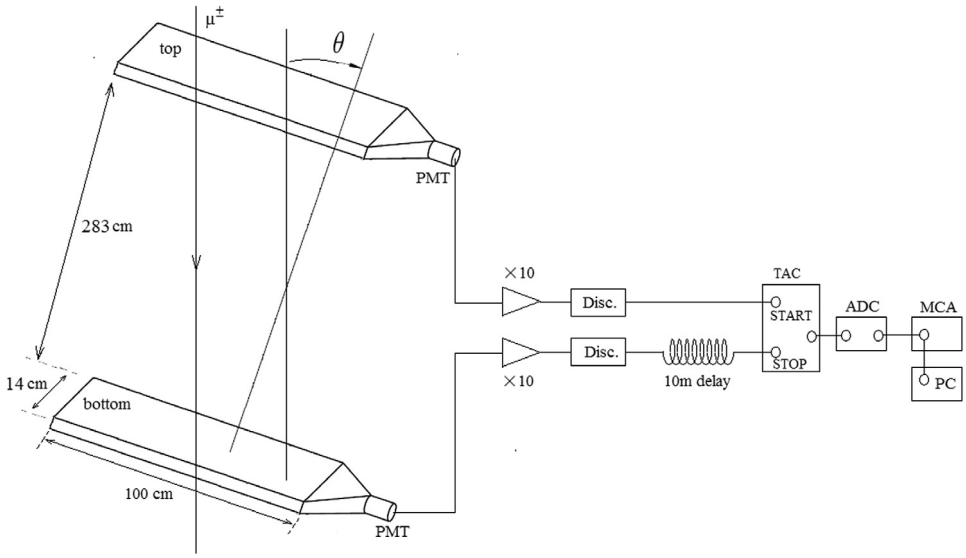

Fig. 3. Schematic view of cosmic ray muons telescope, and electronic circuit.

voltage signal proportional to the time lag between its input signals. The output from top scintillation detector was sent directly to the START line of the TAC, while the signal from the bottom one, delayed by ∼50 ns using a 10 m coaxial and LEMO cable, was sent to the STOP line. Eventually, the TAC output is fed into a multichannel analyzer (MCA) via an analog to digital converter (ADC) unit. In this way, by passing a particle from two scintillators, the time lag between the signals produced in the two top and bottom scintillators is recorded by a computer.

The telescope is equipped to measure the muon flux at various zenith and azimuth angles. The acceptance of this telescope is ≈26 cm^2 sr.

Muons lose their energy by passing through the materials. The average energy lost per unit length, $\frac{dE}{dx}$, for any charged particle passing through a matter is obtained by the Bethe–Bloch equation [9]. The telescope used in this experiment consists of two scintillators each one with a thickness of 10 mm. To obtain the minimum energy of the muons passing through the telescope, the muon should be transmitted perpendicularly to the surface of the scintillators and must pass through a 10 mm thick of the top scintillator and stop at about 1 mm in the bottom scintillator. Using a Monte Carlo program, a muon with a kinematic energy equal to the rest energy of muon is taken. Then, Δx = 0.1 mm steps are taken in the direction of the back track. In the first step, the energy $\Delta E = \frac{dE}{dx}\Delta x$ is added to the muon. With this new energy, the new value of $\frac{dE}{dx}$ is computed, and another energy value is added to the muon. Eventually, when the muon reaches the beginning of its path in the telescope, the sum of the energies added to it is calculated. This energy is the minimum energy required for a muon to record an event. The calculated minimum energy is 0.76 GeV.

4. Experimental data and their analysis

The muon fluxes in the North, West, South, and East directions and in 3 zenith angles of $20° \pm 10°, 40° \pm 10°$ and $60° \pm 10°$, in total from 12 directions were measured. Total measurements were done in 288 h (for each situation, 24 h). To properly compare the time difference spectra in different directions, it is necessary all experimental conditions, except the telescope direction, is the same. Hence, the voltages, thresholds, and other electronic adjustments were kept untouched. The atmospheric conditions should be also considered, since these produce substantial modulations in the muon rate. The meteorological records from the Mehrabad weather station shows the local pressure and temperature vary at different times of a day, but their values are almost identical at similar times in different days. Since the experimental time for each direction of the telescope is within 24 h and these experiments were performed at similar times, the pressure and temperature effects have not been shown to correct the data in these experiments. Time lag spectra of muon events recorded in different directions are shown in Fig. 4. Each count in these spectra corresponds to passing a particle from the top and bottom scintillators (Fig. 3). The peak of the spectrum is to correspond to the mean time of flight between scintillator paddles top and bottom for muons passing through the telescope. The width of the muon time distribution has several sources. These sources include the variance in path length of muons between two scintillator paddles, thermal noise, jitter in the electronics, variance in the lengths of paths of propagation within the scintillator paddles, various velocities of muons (Eq. (8)), and other sources of uncertainty. In effect, these multiple sources are combined to give a total effective width for our timing distributions. To determine the total number of muons in each spectrum, we obtain the number of counts in the peak region by subtracting the background counts, which is calculated from the distant regions. Table 1 shows the total counts in the spectra for different directions.

Table 1
Total count of muons for different directions.

Zenith angle	20°	40°	60°
North	19 422 ± 142	13 012 ± 116	5658 ± 79
West	20 312 ± 145	13 046 ± 127	5701 ± 87
South	19 206 ± 140	13 013 ± 118	5698 ± 78
East	17 349 ± 145	11 238 ± 118	5414 ± 85

Table 2
Mean time-spacing between two successive muon events, τ, for different directions.

Zenith angle	20°	40°	60°
North	4.1 s	5.9 s	12.2 s
West	3.8 s	6.1 s	13.1 s
South	4.1 s	5.7 s	14.9 s
East	4.6 s	7.0 s	14.9 s

The time interval distribution between two consecutive muon events in case of $\theta = 20°$, and $\phi = 0°$ is demonstrated in Fig. 5. Due to the randomness of the event time, we expect this distribution to follow the exponential distribution function, as $f(t) = f(0)e^{-t/\tau}$. Mean time interval can be found by fitting the function $f(t)$ on time interval distribution. Table 2 shows the different values of τ for the different directions. In fact, these values represent the mean time-spacing between two consecutive muon events.

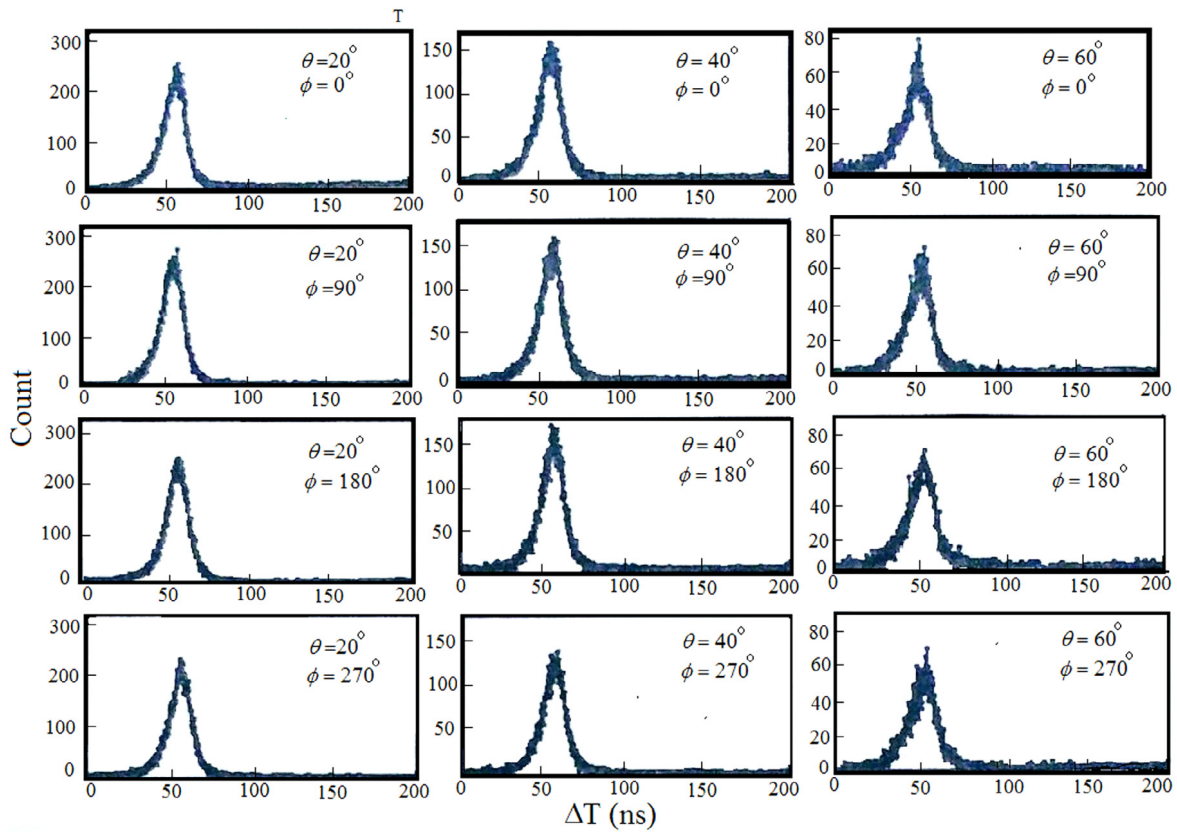

Fig. 4. Time lag spectra of muon events recorded in different directions.

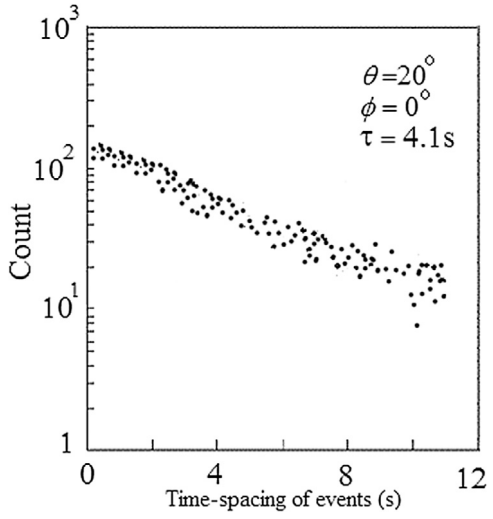

Fig. 5. Time-spacing distribution of successive muon events.

Table 3
Muon events flux (in m^{-2} s^{-1} sr^{-1}) for different directions.

Zenith angle	0°	20°	40°	60°
North	105.8 ± 0.7	91.9 ± 0.7	61.6 ± 0.6	26.8 ± 0.4
West	105.8 ± 0.7	96.1 ± 0.7	64.7 ± 0.6	27.0 ± 0.4
South	105.8 ± 0.7	90.9 ± 0.6	61.5 ± 0.5	26.9 ± 0.4
East	105.8 ± 0.7	82.1 ± 0.7	53.1 ± 0.5	25.6 ± 0.4

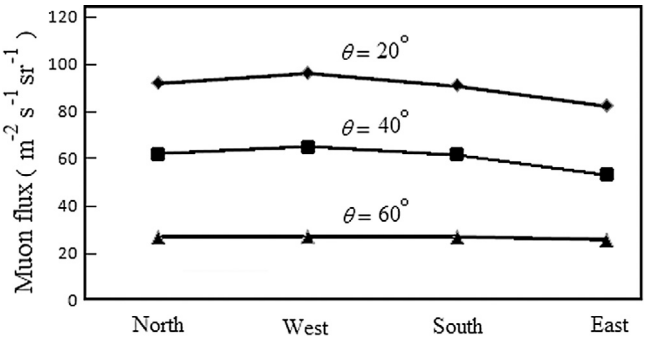

Fig. 6. Azimuthal angular dependence of the muon events for different zenith angles.

The muon flux can be obtained by the following equation,

$$F_\mu = \frac{Rd^2}{A_{top}A_{bottom}}. \quad (9)$$

where R is count rate of muons, d distance between two scintillator paddles, and A_{top} and A_{bottom} are surface areas of the top and bottom scintillators respectively. The muon flux in different directions is shown in Table 3. To complete the measurements, the muon flux along the vertical axis ($\theta = 0°$) was also measured. The value of this flux is given in Table 3, as well. In addition, azimuthal angular dependence of the muon events for different zenith angles, θ = 20°, 40°, and 60°, is shown in Fig. 6. An asymmetry can be seen in East–West direction. The West–East asymmetry can be shown using the amplitude of $2(f_W - f_E)/(f_W + f_E)$, where f_W and f_E show the flux of muons in west and east direction respectively. The standard deviation σ is obtained as:

$$\sigma = \frac{4}{(f_W + f_E)^2}(f_E^2 f_W + f_W^2 f_E)^{0.5}. \quad (10)$$

These amplitudes are about 0.157 ± 0.010, 0.197 ± 0.013, 0.053 ± 0.019 for zenith angle θ = 20°, 40°, and 60° respectively.

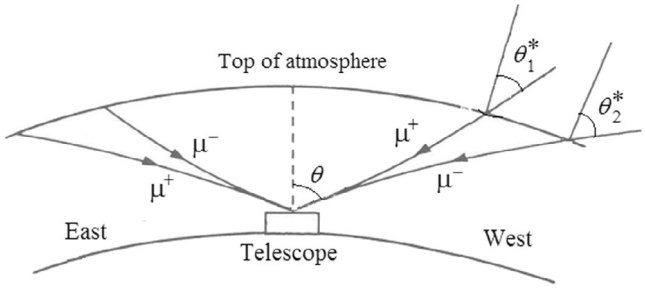

Fig. 7. Schematic description of the East–West effect of atmospheric muons.

The East–West effect, whose details have been investigated in numerous studies for example in [10–13], is actually the interaction of the geomagnetic field with secondary charged particles, especially with muons [14–16]. Fig. 7 shows a schematic description of this effect on muons. Positive and negative muons which are observed with a telescope under a particular zenith angle θ, have been produced from different showers due to the different bending in the geomagnetic field due to the different charge signs. The bending of muons depends on their movement in the east or west directions. In fact, low-energy muons are deflected in the geomagnetic field at large Zenith angles. The angle of deflection is approximately as.

$$\alpha = \frac{X}{R}. \tag{11}$$

Here X and R are the path length and curvature radius of a muon, respectively. For a muon with momentum, p, and total energy, E, the radius of curvature in the magnetic field, B, is $R = \frac{pc}{ecB} \approx \frac{E}{ecB}$. For a magnetic field $B \approx 0.5 \times 10^{-4}$T, the curvature radius in meters is $R \approx 0.67 \times 10^5(\frac{E}{1\ \text{GeV}})$. So for a muon with energy 1GeV and zenith angle $\theta = 20°$, and with a vertical altitude of atmosphere $h_v = 10$ km, the deflection angle is about $\alpha \approx 0.16$ rad $\approx 9°$. In the west direction, the path length of a positive muon is shorter than a negative muon. So the positive and negative muons that enter the telescope in the same zenith angle θ, in fact they were produced in different zenith angles, respectively, $\theta_1^* = \theta - \alpha$ and $\theta_2^* = \theta + \alpha$ at top of the atmosphere as shown in Fig. 7. Thus from one side, the number of atmospheric positive muons is more than the negative muons, and from the other side at a certain angle, the path length of positive muons is less than the negative muons in the west direction relative to the east. Therefore, these features indicate, how the different bending of the trajectories of positive and negative muons in the geomagnetic field causes a West–East effect.

The differential zenith angle distribution of atmospheric muons is shown in Fig. 8. The atmospheric muons flux depends on the zenith angle, θ, as:

$$f(\theta, h_v, E) = f(0°)\cos^{n(h_v,E)}(\theta). \tag{12}$$

where h_v is the vertical length of the muon path and E the muon energy. In our experiments the zenith angle distribution of the cosmic ray muon flux integrated on all azimuth angles (Table 3) can be represented by Eq. (13) with $n = 2.03 \pm 0.08$.

The telescope used in this experiment has a large aperture and wide field of view. This means that if the telescope's axis is along the angle θ, then all the muon count is only not related to this angle. To determine the effective angle of the telescope, which is important for obtaining the zenith angle distribution of muons, two factors must be taken into account.

(1) The first factor is the effective surface area of the telescope for each angle. When the axis of the telescope is along the angle θ, we have the most effective surface area, but by increasing or decreasing this angle, the effective area decreases.

(2) The second factor is the intrinsic reduction of muons with the zenith angle in the atmosphere, given by the relation $\cos^n\theta$.

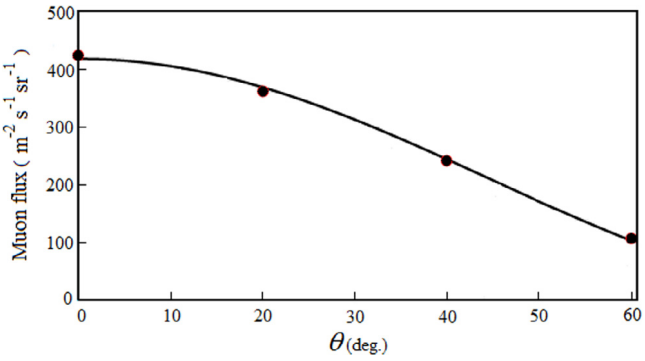

Fig. 8. Zenith angle distribution of atmospheric muons.

Table 4
Angle correction with iteration method.

j	$n^{(j)}$	θ_1 (deg.)	θ_2 (deg.)	θ_3 (deg.)
0	2.03 ± 0.08	20.0	40.0	60.0
1	2.24 ± 0.09	23.0	39.8	56.6
2	2.31 ± 0.11	22.8	39.4	55.8
3	2.33 ± 0.11	22.8	39.3	55.6
4	2.33 ± 0.11	22.8	39.3	55.6

We investigate the effect of these two factors as follows:

The surface of the top scintillator paddle is divided into small square elements, 0.5×0.5 cm^2, and all possible directions for entering a particle into each of these elements and passing through the bottom scintillator paddle are found, and in each case, the incidence angle relative to the zenith axis is calculated. In this way, for all the square elements on the surface of the top scintillator, the frequency of the zenith angles recorded by the telescope is obtained. This frequency shows the distribution of the effective surface area of the telescope in terms of angle θ. Fig. 9 shows the distribution, $S(\theta)$, for three different states of detector. As can be seen, the peaks of these distributions are at angle between the axis of the telescope with the zenith.

The effective angle of the telescope in each position is calculated by considering the distribution function of the telescope effective surface area, $S(\theta)$, and the inherent distribution of the incident particles, $\cos^n\theta$. Using the iteration method, we first assume that the flux of muon events is at the same angles of $\theta_1^{(0)} = 20°$, $\theta_2^{(0)} = 40°$, and $\theta_3^{(0)} = 60°$, and the function $\cos^n\theta$ is fitted on these points and the parameter n is found. The values of the mean angles in various states of telescope are calculated by taking the weight functions into account as follows:

$$\theta_i^{(1)} = \frac{\int_{\theta_i-20°}^{\theta_i+20°} \theta[S(\theta)\cos^{n^{(0)}}\theta]sin\theta d\theta}{\int_{\theta_i-20°}^{\theta_i+20°} [S(\theta)\cos^{n^{(0)}}\theta]sin\theta d\theta}; \qquad i = 1, 2, 3. \tag{13}$$

With new $\theta_i^{(1)}$ ($i = 1, 2, 3$), and with the re-fitting of the function $\cos^n\theta$, the new value of $n^{(1)}$ is obtained, and this is repeated so that $n^{(j)}$ converges to a certain value. Table 4 presents this process. The final value is $n = 2.33 \pm 0.11$.

5. Finding n using simulation

With 3×10^5 air showers produced by proton, alpha, and carbon with fractions of 87, 12, and 1 percent respectively, the zenith angle distribution of muons at Tehran's level is obtained for 20 energy intervals. the value of $n(h_v, E)$ can be obtained by fitting the function of Eq. (12) over this distribution. Fig. 10 shows the values of this parameter for different energies, with bin width of 5GeV, at Tehran's level. The values of this parameter at Tehran's level can be displayed by the function $n(h_{Tehran}, E) = n_0 + n_1\ln(E/\text{GeV}) + n_2\ln^2(E/\text{GeV})$, with $n_0 = 3.8162 \pm 0.0751$, $n_1 = -0.9676 \pm 0.0522$, $n_2 = 0.0671 \pm 0.0086$, and with a regression 99.5%. As can be seen, the parameter n decreases with

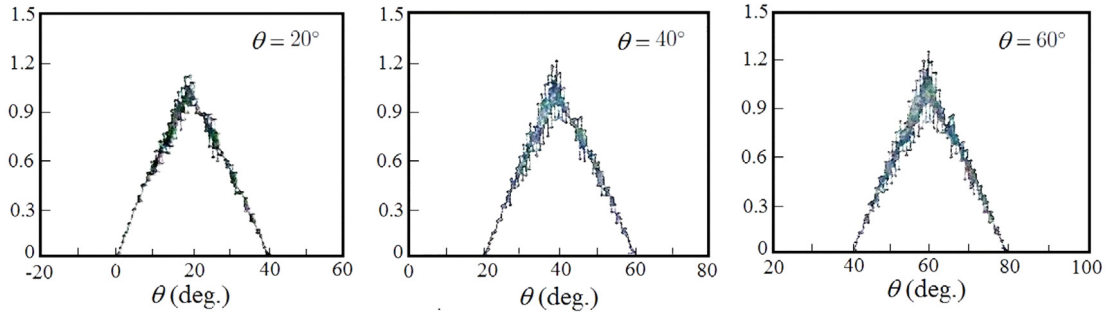

Fig. 9. Distribution of the effective surface area of the telescope in different directions.

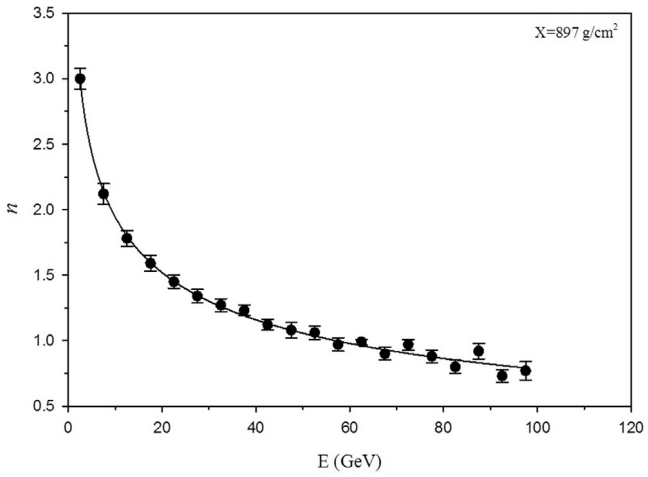

Fig. 10. The value of the parameter n for different energies at Tehran's level.

Table 5
The values of the parameter $n(E)$ in different energies at Tehran's level.

E (GeV)	n
2.5 ± 2.5	3.00
7.5 ± 2.5	2.12
12.5 ± 2.5	1.78
17.5 ± 2.5	1.59
22.5 ± 2.5	1.45
27.5 ± 2.5	1.34
32.5 ± 2.5	1.27
37.5 ± 2.5	1.23
42.5 ± 2.5	1.12
47.5 ± 2.5	1.08
52.5 ± 2.5	1.06
57.5 ± 2.5	0.97
62.5 ± 2.5	0.99
67.5 ± 2.5	0.90
72.5 ± 2.5	0.97
77.5 ± 2.5	0.88
82.5 ± 2.5	0.80
87.5 ± 2.5	0.92
92.5 ± 2.5	0.73
97.5 ± 2.5	0.77

increasing energy. This indicates that with increasing energy, the zenith angle distribution of the muons becomes softer. In fact, reducing the number of muons at large zenith angles in low energy is more than high energy. Table 5 shows the values of the parameter $n(h_v, E)$ in different energies at Tehran's level. With the distribution function of Eq. (6) we can obtain the mean value of n as below.

$$\bar{n} = \frac{\Sigma_{i=1}^{20} n_i(E) \frac{dN}{dE}}{\Sigma_{i=1}^{20} \frac{dN}{dE}} = \frac{\Sigma_{i=1}^{20} n_i(E) \frac{(E_0+E)^{-\eta}}{1+\frac{E}{\epsilon}}}{\Sigma_{i=1}^{20} \frac{(E_0+E)^{-\eta}}{1+\frac{E}{\epsilon}}} \tag{14}$$

with $E_0 = 9.8 \pm 0.3$ GeV, $\eta = 2.5 \pm 0.1$, and $\epsilon = (8 \pm 2) \times 10^3$ GeV, and with the values $n_i(E)$ given in Table 5, we obtain $\bar{n} = 2.30 \pm 0.10$. There is a good match between the experimental value, $n = 2.33 \pm 0.11$, and the simulation value, $\bar{n} = 2.30 \pm 0.10$. This indicates that the method used in analyzing experimental data is a suitable method.

6. Concluding remarks

Zenith and Azimuth angle distributions of atmospheric muons are obtained by using a cosmic ray telescope at Sharif University of Technology in Tehran (35°43′N, 51°20′E, 1200 m a.s.l. ≡ 897 g cm^{-2}). The minimum energy of atmospheric muons, which is determined by energy dissipation in the scintillator paddles of the telescope using the Bethe–Bloch formula, is about 0.76 GeV. The distribution of the time interval between two successive muon events is followed by an exponential law, $e^{-t/\tau}$, indicating the randomness of these events. The muon fluxes have been obtained in 12 different states including the north, west, south, and east directions, and along the zenith angles of the 20°, 40°, and 60°. An anisotropy along the East–West (known as the East–West effect) is seen in the flux of the muons, which is related to the geomagnetic field. The amplitudes of this anisotropy, $2(f_W - f_E)/(f_W + f_E)$, are about 0.157 ± 0.010, 0.197 ± 0.013, 0.053 ± 0.019 for zenith angles $\theta = 20°$, 40°, and 60° respectively. The zenith angle distribution of atmospheric muons obeys a function $\cos^n \theta$, with $n = 2.33 \pm 0.11$.

Also with 3×10^5 air showers generated by proton, alpha, and carbon with CORSIKA code we obtained the value n for 20 energy intervals. The mean value $\bar{n} = 2.30 \pm 0.10$ has a good match with the experimental result. Despite similar experiments performed in the past, the results of this experiment are unique for a height of 1200 m above sea level. In addition, the proposed method for finding value n with experimental data is a suitable method. Meanwhile this is an easy method that can be used by any other group for its specific experimental tool.

Acknowledgments

I would like to thank Ms Saba Mortazavi Moghaddam for all her meritorious helps. This work was supported by the office of vice president for science, research and technology of Sharif University of Technology, Iran.

References

[1] T.K. Gaisser, Cosmic Rays and Particle Physics, Cambridge Univ. Press, New York, 1990.
[2] M. Bahmanabadi, F. Sheidaei, M. Khakian Ghomi, J. Samimi1, Phys. Rev. D 74 (2006) 082006.
[3] See theoritical e.g. C. Stormer, Z. Astrophys. 1 (1930) 237;
W.F.G. Swann, Phys. Rev. 44 (1933) 224;
K.G. Malmfors, Ark. Mat. Astron. Fys. A 32 (section IV) (1945) 29;
R.A. Alpher, J. Geophys. Res. 55 (1950) 437.
[4] D. Heck, et al., Report FZKA6019 (Forschungszentrum Karlsruhe), 1998.

[5] N.N. Kalmykov, S.S. Ostapchenko, Yad. Fiz. 56 (1993) 105; Phys. At. Nucl. 56 N3 (1993) 346.
N.N. Kalmykov, S.S. Ostapchenko, A.I. Pavlov, Izv. RAN Ser. Fiz. 58 N12 (1994) 21;
N.N. Kalmykov, S.S. Ostapchenko, A.I. Pavlov, Bull. Russ. Acad. Sci. Phys. 58 (1994) 1966;
N.N. Kalmykov, S.S. Ostapchenko, A.I. Pavlov, Nucl. Phys. B(Proc. Suppl.) 52B (1997) 17.
[6] H. Fesefeldt, (GHEISHA), RWTH Aachen, Germany Report No. PITHA-85/02 (1985 (unpublished)).
[7] https://www.ngdc.noaa.gov/geomag-web/.
[8] J. Xu, et al., Materials 11 (6) (2018) 944.
[9] C. Grupen, Astroparticle Physics, Springer-Verlag Berlin Heidelberg, 2005.
[10] J. Wentz, et al., J. Phys. G: Nucl. Part. Phys. 27 (2001) 1699;
J. Wentz, et al., Phys. Rev. D 67 (2003) 073020.
[11] P. Lipari, T. Stanev, T.K. Gaisser, Phys. Rev. D 27 (1998) 073003.
[12] C. Stormer, Astrophysics 1 (1930) 237.
[13] J. Wentz, A. Bercuci, B. Vulpescu, Proc. 27th ICRC, Hamburg, 3, 2001, p. 1167.
[14] O.C. Allkofer, et al., J. Geophys. Res. 90 (1985) 3537.
[15] T. Futagami, et al., Super-Kamiokande Collaboration, Phys. Rev. Lett. 82 (1999) 5194.
[16] P. Lipari, Astropart. Phys. 14 (2000) 171.